

Using transcriptomic data to improve the prediction of immunity traits in pigs



T. Jové-Juncà ^a, V.P. Haas ^{b,c}, M.P.L. Calus ^b, M. Ballester ^a, R. Quintanilla ^{a,*}

^a IRTA, Animal Breeding and Genetics, Torre Marimon, 08140 Caldes de Montbui, Spain

^b Wageningen University and Research, Animal Breeding and Genomics, Droevedaalsesteeg 4, 6708 PB Wageningen, the Netherlands

^c University of Hohenheim, Institute of Animal Science, 70599 Stuttgart, Germany

ARTICLE INFO

Article history:

Received 21 July 2025

Revised 5 December 2025

Accepted 8 December 2025

Available online 16 December 2025

Keywords:

Best Linear Unbiased prediction

Genomic prediction

RNA sequencing

Robustness

Swine

ABSTRACT

Considering health-related traits among breeding selection criteria has been proposed as a way to improve pig robustness. This study investigated the potential of whole blood RNA-sequencing data for predicting immunity-related traits, stress indicators and carcass weight, using data from 255 pigs belonging to a commercial Duroc population. The prediction performance of mixed models fitting either genomic (G), transcriptomic (T) or both effects as independent (GT) was evaluated and compared. Three additional models addressing the redundant information between G and T were also evaluated: the GTC model that subtracts the genetic effect from the transcriptome, the GTCi model that makes this correction based on the estimated heritability of T effects, and a multiomic model that weights G and T effects in a multiomics relationship matrix. The models including gene expression information captured a higher proportion of variance than the genomic model for all studied traits but carcass weight. Adding transcriptomic effects improved both model fit and phenotypic prediction of all immunity traits, particularly those with a high transcriptomic contribution such as the abundance of T helper and $\gamma\delta$ T cells, the haptoglobin concentration and the leukocyte counts. Considering the interaction between genomic and transcriptomic effects led to greater prediction accuracies, with the GTCi model performing the best. Our work demonstrates the value of considering gene expression data to predict immunity traits as well as the importance of adequately modelling the interaction between genomic and transcriptomic effects.

© 2025 The Author(s). Published by Elsevier B.V. on behalf of The animal Consortium. This is an open access article under the CC BY-NC-ND license (<http://creativecommons.org/licenses/by-nc-nd/4.0/>).

Implications

Immunity-related traits could be considered in pig breeding programmes to improve animal robustness. Including gene expression data into genomic prediction models could contribute to better predictions of these traits but poses challenges regarding modelling several omics data. The present study confirms the potential of the blood transcriptome data to accurately predict relevant immunity phenotypes in swine and provide key insights about how modelling the overlap between genomic and transcriptomic effects. These results open the possibility of considering expression panels in breeding programmes to improve the porcine immunity profile.

Introduction

Improving animal robustness and resilience against biotic stress factors is an increasingly important goal in pig breeding. Increasing disease resistance has been traditionally approached by finding biomarkers of resistance to specific pathogens and incorporating them into breeding programmes. Immunity parameters have been proposed as indicators of animal immune capacity and robustness ([Visscher et al., 2002](#)), and its genetic determinism has been proved with medium to high heritability estimates ([Ballester et al., 2020, 2023; Roth et al., 2022; Flori et al., 2011](#)). Thus, considering immunity traits into breeding programmes to improve general immunocompetence, as proposed by [Knap and Bishop \(2000\)](#) and [Visscher et al. \(2002\)](#), could be an alternative way to increase animal robustness and disease resistance.

Selection based on such immunity parameters would rely on adequate models to accurately predict breeding. The inclusion of genomic data into models for genetic evaluation of complex traits has been proved to increase the accuracy of predicted breeding values ([Misztal et al., 2020](#)). In addition, developments in high-

* Corresponding author.

E-mail address: raquel.quintanilla@irta.cat (R. Quintanilla).

throughput molecular technologies make it more feasible and affordable to include additional omics data layers such as gene expression data into predictive models. Different approaches for considering transcriptomics data in genomic prediction models have been proposed (Hu et al., 2022; Legarra and Christensen, 2022; Liu et al., 2022; Perez et al., 2022; Li et al., 2019). Most implementations of these approaches have focused on the accuracy of trait prediction (Morgante et al., 2020; Li et al., 2019; Schrag et al., 2018; Takagi et al., 2014), but the inclusion of another layer of information was also expected to improve the prediction of breeding values (Perez et al., 2022).

One main issue in the inclusion of transcriptomics data into predictive models lies in the overlap between transcriptomic and genetic effects. As transcript expression levels are impacted by genetics (Cheung et al., 2003), considering both effects into the model may introduce redundant information, which may result in biased predictions (Michel et al., 2021). Several modelling strategies have been proposed to manage the genetic overlap amongst omics data layers. Christensen et al. (2021) tried a two-step modelling strategy in which transcriptomic variance was calculated after all genomic variance component had been removed. Alternatively, Perez et al. (2022) proposed correcting the transcriptomic relationship matrix by conditioning it on the genotypes, using the genomic heritability, i.e. the proportion of phenotypic variance explained by the genomic component. This method was later revised by Haas et al. (2025), who showed that, instead, the heritability of the transcriptomic effects should be used. A more direct approach was proposed by Liang et al. (2022), in which the contributions of genomics and transcriptomics data to a multi-omic effect were identified based on the better fit of the model.

The present study aimed to predict immunity traits using mixed models incorporating two layers of omics data, genomics and transcriptomics, and to evaluate the potential gain in predictive ability resulting from the inclusion of transcriptomic information. Several mixed models and strategies for considering the covariance between genomic and transcriptomic covariates were considered.

Material and methods

Animal material

The analysed data come from a population of 255 healthy piglets (129 females and 126 males) from a commercial Duroc population. These animals belonged to six commercial batches, each containing between 37 and 46 individuals. Animals were fed *ad libitum* with a cereal-based diet and were all raised in the same farm. Hair and blood samples were collected at 60 ± 8 days of age. Blood was collected from the external jugular vein for both immunity phenotyping and genomic and transcriptomic analyses. Details about hair collection, blood extraction and samples management can be found in Ballester et al. (2020).

Traits

A group of 13 health-related traits, representative of both innate and adaptive immunity, was selected from all traits measured in the population (Ballester et al., 2020, 2023). The studied traits included the concentration of immunoglobulins, acute phase proteins, stress indicators, leukocyte subpopulations, cell counts and phagocytosis capacity. Moreover, carcass weight was also considered as a representative production-related trait, measured at a different time.

Total concentrations of immunoglobulins G and M, as well as C-reactive protein (CRP), were obtained by ELISA (Bethyl Laboratories Inc., Bionova, Spain and Abcam Plc., Spain) from plasma and

serum samples, respectively. Absorbance was read using an ELISA plate reader (Bio-Rad) and bioinformatically analysed with Microplate manager 5.2.1 software (Bio-Rad). Haptoglobin (HP) concentration was obtained from serum samples using colorimetric assays (Tridelta Development Limited, Ireland). For phagocytosis measurements, whole blood samples were incubated with fluorescein-labelled opsonised *E. coli* (BD Pharmigen, Spain) and analysed with flow cytometry using the MACSQuant Analyzer 10 Flow cytometer (Miltenyi Biotec GmbH, Bergisch Gladbach, Germany) with the appropriate software MACSQuantify software v2.6 (Miltenyi Biotec GmbH, Bergisch Gladbach, Germany), obtaining the percentage of cells presenting % of phagocytic cells as well as the fluorescence intensity (measure of phagocytic uptake). Different leukocyte subpopulation levels were quantified by performing a hemogram on blood samples using CELL-DYN® 3700 (Abbott, Spain) in the Laboratory Echevarne (Spain; Barcelona); in this study, we analysed lymphocyte, monocyte, and total leukocyte counts. Peripheral blood mononuclear cells were extracted using gradient centrifugation with Histopaque-1077 (Sigma, Spain); the peripheral blood mononuclear subpopulations analysed in this study, such as $\gamma\delta$ T cells and T helper cells, were quantified by immunolabelling with specific monoclonal antibodies. The $\gamma\delta$ T cells were quantified using APC Rat Anti-Pig $\gamma\delta$ T Lymphocytes (MAC320 clone, BD Biosciences, Spain). T helper cells (CD3+CD4+CD8-) were labelled with Fluorescein emission Mouse Anti-Pig CD8 α (76-2-11 clone), Alexa Fluor® 647 Mouse Anti-Pig CD4 α (74-12-4 clone) and PE-Cy™7 Mouse Anti-Pig CD3 ϵ (BB23-8E6-8C8 clone) (BD Biosciences, Spain). Stained cells were analysed by flow cytometry using a MACSQuant Analyzer 10 Flow cytometer (Miltenyi Biotec GmbH, Bergisch Gladbach, Germany) and the Flowlogic™ software v7.3 (Inivai Technologies, Melbourne, Australia). Stress parameters were also considered: cortisol concentrations in blood and hair were measured using targeted liquid chromatography-tandem mass spectrometry and an ELISA kit (Cusabio Technology LLC., Bionova, Spain), respectively; for more details about the hair extraction and the characterisation of T cell subpopulations, refer to Ballester et al. (2020; 2023). Finally, traceability of these animals was maintained during growing and fattening periods, and hot carcass weight was measured at slaughter, at an average weight of 129 kg and 180 days of age.

The normality of all phenotypes was assessed using the Shapiro-Wilk test and phenotypes were adjusted using log2 transformation when required to reach normality, which was the case for all phenotypes with the exception of immunoglobulin M concentration, % of phagocytic cells and carcass weight. Exceptionally, the cortisol concentrations in hair and blood did not achieve normality after log transformation; therefore, a square root transformation was applied, which achieved normality. The impact on each of the phenotypes of three potential co-factors, sex, batch and date of laboratory analyses was evaluated through linear models performed with the base R lm function. Those co-factors with a significant impact on a specific trait were considered in subsequent models.

Genotypes

Genomic DNA was isolated from blood samples using NucleoSpin Blood (Macherey-Nagel, Germany). Sample purity was assessed with a Nanodrop ND-1000 spectrophotometer. From the isolated DNA, genotypes for 68 516 single-nucleotide polymorphisms (SNPs) were obtained using the GGP Porcine HD Array (Illumina, San Diego, CA) using the Infinium HD Assay Ultra protocol (Illumina). Genotype quality control was performed using Plink v1.90b3.42 (Purcell, 2007) and was set to eliminate genotypes with a minor allele frequency less than 0.05 or with more than 10% missing genotype data. After filtering, 42 641 SNPs remained.

The resulting genotypes were submitted to an imputation pipeline departing from a multibreed Pig Genomics Reference Panel from PigGTEX (Teng et al., 2022), which included 1 602 whole-genome sequence samples covering over 100 pig breeds. A total of 42 M autosomal biallelic SNPs were considered for imputation. The imputation procedure was performed using Beagle v5.1 (Browning et al., 2018). SNPs with a dosage R-squared > 0.8 were considered properly imputed and selected. Afterwards, the same filters of minor allele frequency below 0.05 and missing data above 10% were applied. A total of 8 499 177 SNPs remained after filtering, with an accuracy of imputation of $R^2 = 0.91$.

Gene expression levels

RNA was extracted from whole blood samples using TempusTM Spin RNA Isolation Reagent Kit (Thermo Fisher Scientific, Spain). Concentration, purity and integrity of the isolates were measured using a Nanodrop ND-1000 spectrophotometer and Fragment Analyzer (Agilent Technologies Inc., Santa Clara, CA), respectively. All samples had a RNA integrity number value greater than 8. Globin and ribosomal depletion were performed using Ribo-Zero Plus rRNA depletion (Illumina), creating the libraries to be sequenced.

RNA sequencing was performed with an Illumina NovaSeq6000 platform at Centro Nacional de Análisis Genómico (CNAG-CRG, Barcelona, Spain). Sequencing depth was set at > 55M with paired-end reads. FastQC software (Wingett and Andrews, 2018) was used to perform quality control. Mapping was performed using STAR 2.75.3a software (Dobin et al., 2013) against the reference *Sscrofa11.1* genome assembly with the Ensembl Genes 109 annotation database. Quantification of gene counts was performed with RSEM 1.3.0 software (Li and Dewey, 2011).

Raw counts were then normalised with the EdgeR R package (Robinson et al., 2009) using the trimmed mean on M-values, followed by a log2 transformation. Minimum expression thresholds were established at expression in less than 5% of the population and an average count inferior to 0.69 counts per million. Normality was tested using the Shapiro-Wilk test with a leave-one-out approach, which allowed for the detection and subsequent removal of outliers. A total of 16 063 genes remained after filtering.

Prediction models incorporating transcriptomic effects

Several prediction models using omics data were used, all based on the basic animal model for BLUP. In the following section, each model used will be introduced with their particularities and key features. All analyses using mixed linear models were constructed with ASReml R (Version 4.2) (Butler et al., 2023) in R Studio (Version 2025.05.0) (Posit Team, 2025).

Genomic and transcriptomic models

The first model used was the genomic (G) model (VanRaden, 2008) which incorporates the additive genomic relationship matrix to define the genetic similarities between individuals:

$$y^* = X\beta + g + e \quad (1)$$

where y^* stands for the vector of phenotypes, β is the vector of fixed effects (sex and batch) and X is the corresponding incidence matrix, and g stands for the vector of random additive genetic values of all individuals, distributed as $g \sim N(0, G\sigma_g^2)$, G being the additive genomic relationship matrix and σ_g^2 the additive genomic variance. The genomic relationship matrix G was computed as $G = \frac{V}{m}$, where V is the matrix of centred and standardised genotypes for all individuals and m is the number of genotypes. Finally, e is the vector of residual effects, distributed as $e \sim N(0, I\sigma_e^2)$, and σ_e^2 the residual variance.

The transcriptomic (T) model (Guo et al., 2016) considers the transcriptomic instead of the genomic effect, as follows:

$$y^* = X\beta + t + e \quad (2)$$

where t stands for the vector of random transcriptomic effects, distributed as $t \sim N(0, T\sigma_t^2)$, being T the transcriptomic relationship matrix and σ_t^2 the transcriptomic variance. T is described as $T = \frac{WW'}{k}$, where W is the matrix of centred and standardised expression levels for all individuals precorrected by sex and batch and k is the number of genes which expression was factored in.

The genomic and transcriptomic (GT) model (Li et al., 2019) incorporates both genomic and transcriptomic effects, treating g and t as independent random effects:

$$y^* = X\beta + g + t + e \quad (3)$$

where all terms are as defined above in Eqs. (1) and (2).

Models addressing the overlap between genomic and transcriptomic information

Two models described by Perez et al. (2022) and Haas et al. (2025) consider the overlap between genomic and transcriptomic information by conditioning transcriptomic data on SNP genotypes to render them independent, i.e. to correct for the covariance between genomic and transcriptomic effects, on the basis of either the heritability (GTC model) or the heritability of transcript effects (GTCi model). These models are defined as follows:

$$y^* = X\beta + g + t_c + e \quad (4)$$

being t_c the vector of transcriptomic effects conditioned to genotypes, with a conditioned transcriptomic relationship matrix $T_c = \frac{W_c W_c'}{k}$, where W_c can be computed in two different but mathematically equivalent ways (Haas et al., 2025). Here, we used the expression $W_c = (I - G^* + (G^*(I + G^*)^{-1}G^*))W$, which is advised to use if the number of SNPs is (much) larger than the number of genotyped animals (Haas et al., 2025). The G^* matrix is defined here as $G^* = \frac{G \sum_j 2p_j(1-p_j)}{k}$, where p_j stands for the allele frequency of SNP j .

In the GTC model, λ is computed as $\lambda = \frac{m\sigma_g^2}{\sigma_e^2} = m\left(\frac{1}{h_g^2} - 1\right)$, where σ_g^2 and σ_e^2 are the residual and genomic variances estimated from G model, i.e. h_g^2 is the estimated genomic heritability. In GTCi model, a heritability of transcript-level (\tilde{h}_t^2) was estimated iteratively by maximising the log-likelihood of Eq. (4) and considered for computing lambda as $\lambda = \sum 2pq\left(\frac{1}{\tilde{h}_t^2} - 1\right)$. This was done by testing different values of \tilde{h}_t^2 (in steps of 0.001) between 0.045 and 0.995, as described in Haas et al. (2025), and selecting the value that maximised the log-likelihood.

Finally, a multiomic (M) model, described by Liang et al. (2022), considers only a multiomic random effect (m) combining genomic and transcriptomic effects as follows:

$$y^* = X\beta + m + e \quad (5)$$

where the multiomic effect is distributed as $m \sim N(0, M\sigma_m^2)$, and the multiomic relationship matrix M is defined as: $M = r * G + (1 - r)T$, where r is the ratio between the impact of genomic (G) and transcriptomic (T) effects on the trait, taking values between 0 and 1. When $r = 1$, the M model would be equivalent to the G model; when $r = 0$, it would correspond to the T model. Following Liang et al. (2022), the r parameter was iterated by assigning values between 0.045 and 0.995 in increases of 0.001 and the value yielding the highest maximum likelihood was used for subsequent analyses.

Variance components estimation

The variance components for genomic, transcriptomic or multiomic effects on immunity-related and carcass traits under the considered models (G, T, GT, GTC, GTCi and M) were estimated by restricted maximum likelihood using the R package ASReml R (Version 4.2) (Butler et al., 2023). The proportion of total phenotypic variance explained by the random effects under the different models was computed, and the log-likelihood of each model was retained.

From the variance components, the heritability of each trait in models considering genetic effects was calculated as $h^2 = \frac{\sigma_g^2}{\sum \sigma_i^2}$, where σ_g^2 is the genetic variance and $\sum \sigma_i^2$ is the sum of the variances of all random factors included in the model. Similarly, the proportion of transcriptomic variance (t^2) was calculated as $t^2 = \frac{\sigma_t^2}{\sum \sigma_i^2}$, where σ_t^2 is the transcriptomic variance, and $\sum \sigma_i^2$ is defined as above. The r parameter considered in MBLUP was also iterated this way using the same increments and interval of iterated values and selected by maximum likelihood.

Model fit comparison

A likelihood ratio test between models was performed to test the improvement of fit of the model for the different studied traits resulting from the inclusion of either transcriptomic or genomic effects. For all studied traits, models considering the two omics effects (GT, GTC, GTCi) were compared against both G and T models when nested; the T model was not considered nested in models with transcriptomic effects conditioned to genotypes (i.e. GTC and GTCi). The ratio between the log-likelihoods of the compared models, following a chi-square distribution, was computed and tested for significance as described in the ASReml R reference manual (Butler et al., 2023).

Prediction ability of models with transcriptomic effects

The gain in prediction accuracy resulting from the incorporation of several layers of omics data into predictive models was evaluated. A random 90/10 split approach with 500 iterations was used to test the ability of the studied models to predict immunity-related traits and carcass weight. At each iteration, missing values were assigned to the phenotypes of 10% of the population selected at random to create a test subpopulation. For each combination of trait-model, the accuracy of phenotypic prediction was assessed upon the vector of correlations resulting from the 500 iterations, obtaining the mean and the confidence interval of the measure.

Differences in prediction accuracy across the models were computed at each iteration, as proposed by Hothorn et al. (2005) and Schrauf et al. (2021), thus reducing the variability in accuracy due to the random selection of testing samples in the comparison of models. The differences computed across the Markov chains were then used to generate the statistics (mean and 95% confidence intervals) for the prediction accuracy differences between models.

Accuracy of genetic evaluation

The accuracy in predicting the expected breeding values for the different immunity-related traits (i.e. the elements of vector g) was also computed for the different models except for the T and M models (i.e. all models considering separate genetic/genomic effects). A similar ten-fold cross-validation approach as described above was used. The accuracy of genomic prediction was calculated using the correlation between the predicted breeding values (vector g) and the observed phenotypes corrected by fixed effects.

Results

In the present study, we analysed the possibility of including RNA-sequencing data into predictive models for fitting 13 immunity-related traits, including immunoglobulins, acute phase proteins, cortisol concentrations, phagocytic measurements, and the abundance of blood cell subpopulations, as well as carcass weight. Descriptive statistics for the analysed traits are presented in Table 1.

Genetic parameters under multiomic models

The proportion of phenotypic variance of each immunity and carcass trait explained by genomic, transcriptomic or multiomic effects in the analysed models is represented in Fig. 1, whereas Table 2 shows the estimated heritability for each trait obtained from models incorporating different layers of omic data. More details about the variance components estimates and the likelihood values of the different models can be found in Supplementary Table S1. In general, the GTCi model was the model explaining the highest proportion of phenotypic variance for the majority of traits, followed by GTC, M and GT models.

The highest heritability across models (Table 2) was found for $\delta\gamma$ T cells in the G model (0.52). This estimate decreased when transcriptomic data were incorporated into the model (0.22 in GT), but part of this heritability was recovered when the covariance between genome and transcriptome was considered in the

Table 1

Descriptive statistics, normalisation procedure and cofactors for analysed pig immunity-related and carcass traits.

Traits	N	Mean	SD	CV	Normalisation	Cofactors
Immunoglobulin M concentration in plasma (mg/mL)	255	2.28	0.85	0.37	–	sex, batch
Immunoglobulin G concentration in plasma (mg/mL)	255	12.71	4.94	0.39	log2	sex, batch
Haptoglobin concentration in serum (mg/mL)	255	-0.13	0.36	-2.92	log2	sex, batch
C-reactive protein concentration in serum (μ g/mL)	254	2.14	0.31	0.15	log2	sex, batch
Phagocytic cells (%)	255	43.54	8.08	0.19	–	sex, batch, date of analysis
Phagocytic uptake (FITC)	255	0.67	0.03	0.05	log2	sex, batch, date of analysis
Leukocytes count (n/ μ L)	254	4.29	0.14	0.03	log2	sex, batch
Lymphocytes count (n/ μ L)	254	4.06	0.15	0.04	log2	sex, batch
Monocytes count (n/ μ L)	252	2.68	0.20	0.08	log2	sex, batch
T helper cells (% of PBMCs)	234	0.21	0.22	1.07	log2	sex, batch
$\gamma\delta$ T cells (% of PBMCs)	235	0.84	0.30	0.35	log2	sex, batch
Cortisol concentration in plasma (nM)	254	13.97	3.21	0.23	square root	sex, batch
Cortisol concentration in hair (pg/mg)	255	2.19	0.19	0.09	log2	sex, batch
Carcass weight (kg)	245	98.52	11.82	0.12	–	sex, batch

Abbreviations: FITC = Fluorescein emission; PBMC = Peripheral blood mononuclear cells.

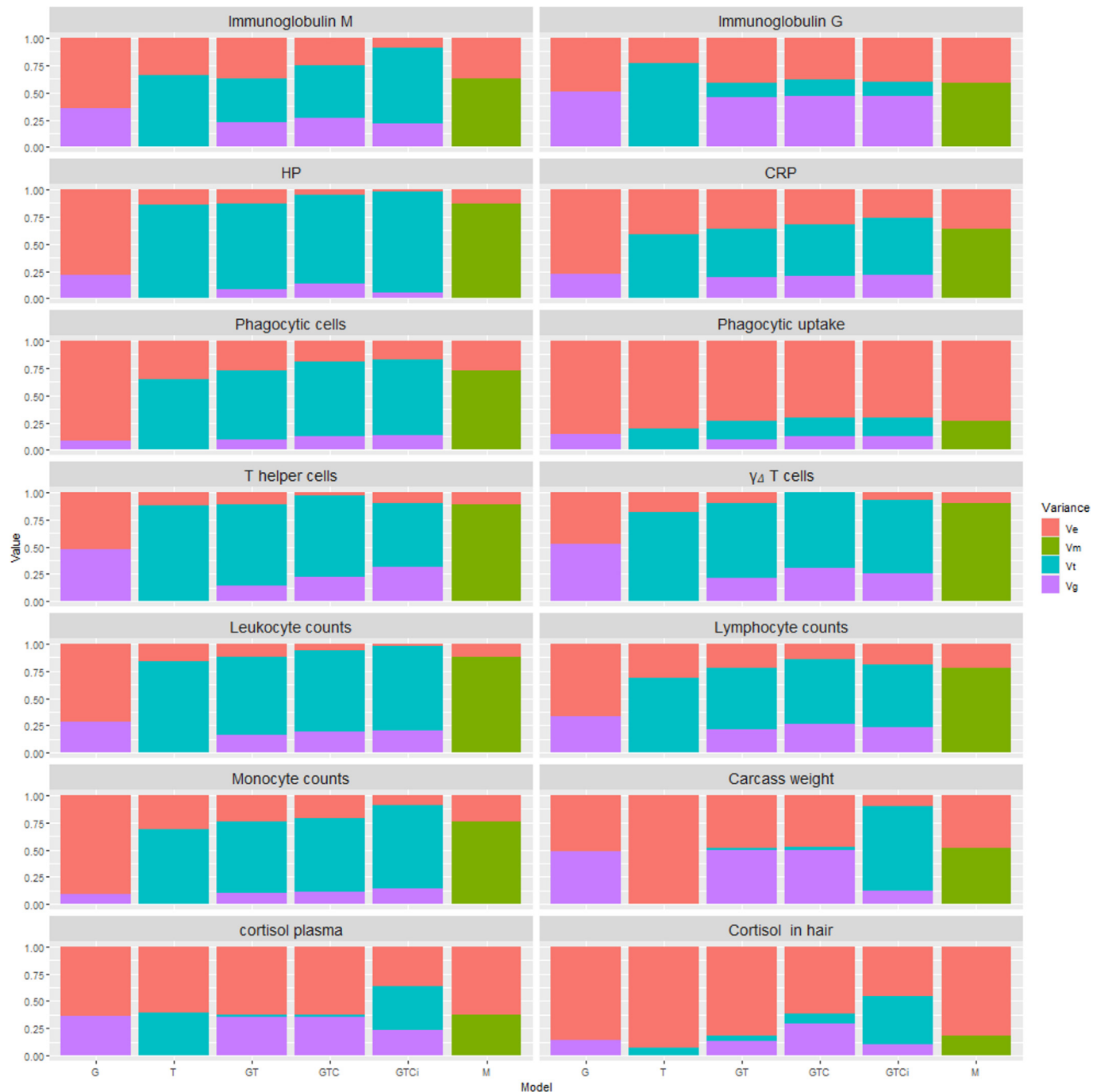


Fig. 1. Stack bar plots showing the percentage of variance components for different immunity traits in pigs across different models: genomic model (G), transcriptomic model (T), genomic and transcriptomic as independent effects (GT), transcriptomics conditioned to genomics on the basis of either the heritability of the trait (GTC) or the heritability of transcriptomic effects (GTCi), and multiomic model (M). The estimated variance components were genetic (Vg), transcriptomic (Vt), multiomic (Vm) and residual (Ve) variances. CRP and HP stand for C-reactive protein and haptoglobin concentrations in serum, respectively.

model (0.31 in GTC). A similar pattern was observed for T helper cell abundance, with heritability estimates ranging from 0.48 (G) to 0.23 (GTC). High heritabilities were also estimated for IgG and carcass weight, but for these traits, the heritability estimates showed little change when transcriptomic data were included in the model. Traits with low heritabilities, such as monocyte count and % of phagocytic cells, presented higher heritabilities in models conditioning the transcripts on the genotypes (i.e. GTC and GTCi). The rest of the traits (immunoglobulin M, HP and CRP concentra-

tions, phagocytic uptake, cortisol concentration in hair, leukocyte and lymphocyte counts) presented medium to low heritabilities, and a slight decrease in the heritability estimate when considering transcriptomic effect, again being the heritability under the GTC model the closest to the heritability under the G model.

The proportion of variance explained by the transcriptomic component of the model (t^2) is shown in Table 2. In the T model, with only transcriptomic effects, t^2 was greater than 0.5 for all analysed traits but phagocytic uptake, cortisol concentrations in

Table 2

Parameter estimates (SD between parentheses) across different models for pig immunity-related and carcass traits. Estimated parameters: heritability (h^2), proportion of variance explained by transcriptomic effects (t^2), heritability of transcriptomic effects (\tilde{h}_t^2), and the ratio between the impact of genomic and transcriptomic effects (r). Models: genomic model (G), transcriptomic model (T), genomic and transcriptomic as independent effects (GT), transcriptomics conditioned to genomics on the basis of either h^2 (GTC) or \tilde{h}_t^2 (GTCi), and multiomic model (M).

Traits	h^2				t^2				\tilde{h}_t^2 GTCi model	r M model
	G model	GT model	GTC model	GTCi model	T model	GT model	GTC model	GTCi model		
Immunoglobulin M in plasma (mg/mL)	0.351 (0.112)	0.227 (0.107)	0.262 (0.088)	0.217 (0.064)	0.660 (0.141)	0.403 (0.139)	0.484 (0.142)	0.692 (0.104)	0.425	0.359
Immunoglobulin G in plasma (mg/mL)	0.505 (0.129)	0.460 (0.131)	0.470 (0.124)	0.466 (0.129)	0.770 (0.144)	0.123 (0.135)	0.151 (0.144)	0.126 (0.136)	0.045	0.787
Haptoglobin in serum (mg/mL)	0.214 (0.118)	0.087 (0.114)	0.137 (0.067)	0.053 (0.022)	0.855 (0.114)	0.783 (0.086)	0.813 (0.099)	0.924 (0.029)	0.867	0.1
C-reactive protein in serum (µg/mL)	0.221 (0.125)	0.196 (0.116)	0.203 (0.104)	0.212 (0.093)	0.588 (0.158)	0.435 (0.148)	0.478 (0.150)	0.528 (0.150)	0.187	0.31
Phagocytic cells (%)	0.087 (0.114)	0.094 (0.096)	0.128 (0.083)	0.137 (0.080)	0.642 (0.128)	0.631 (0.131)	0.674 (0.124)	0.687 (0.121)	0.111	0.13
Phagocytic uptake (FITC)	0.147 (0.128)	0.099 (0.125)	0.122 (0.121)	0.124 (0.121)	0.198 (0.124)	0.165 (0.147)	0.174 (0.154)	0.175 (0.155)	0.075	0.375
Leukocytes count (n/µL)	0.287 (0.129)	0.161 (0.101)	0.191 (0.084)	0.207 (0.074)	0.831 (0.114)	0.719 (0.110)	0.743 (0.110)	0.764 (0.088)	0.184	0.183
Lymphocytes count (n/µL)	0.337 (0.131)	0.212 (0.116)	0.265 (0.098)	0.236 (0.108)	0.690 (0.137)	0.560 (0.127)	0.591 (0.116)	0.572 (0.122)	0.045	0.275
Monocytes count (n/µL)	0.093 (0.105)	0.107 (0.099)	0.116 (0.093)	0.148 (0.068)	0.687 (0.134)	0.653 (0.133)	0.668 (0.130)	0.755 (0.107)	0.215	0.141
T helper cells (% of PBMCs)	0.477 (0.141)	0.141 (0.108)	0.227 (0.076)	0.312 (0.095)	0.878 (0.122)	0.744 (0.121)	0.740 (0.075)	0.587 (0.112)	0.488	0.164
$\gamma\delta$ T cells (% of PBMCs)	0.526 (0.128)	0.219 (0.109)	0.305 (0.035)	0.254 (0.101)	0.818 (0.117)	0.677 (0.111)	0.694 (0.111)	0.677 (0.011)	0.045	0.245
Cortisol concentration in plasma (nM)	0.363 (0.124)	0.351 (0.126)	0.358 (0.124)	0.235 (0.167)	0.397 (0.164)	0.025 (0.126)	0.022 (0.129)	0.398 (0.304)	0.894	0.935
Cortisol concentration in hair (pg/mg)	0.143 (0.104)	0.135 (0.104)	0.143 (0.103)	0.099 (0.071)	0.075 (0.075)	0.052 (0.114)	0.087 (0.120)	0.444 (0.242)	0.823	0.72
Carcass weight (kg)	0.489 (0.136)	0.498 (0.135)	0.500 (0.135)	0.127 (0.129)	0.001 (0.033)	0.013 (0.138)	0.024 (0.141)	0.771 (0.130)	0.955	0.974

Abbreviations: FITC = Fluorescein emission; PBMC = Peripheral blood mononuclear cells.

hair and in blood, and carcass weight. The highest t^2 obtained with the T model was for the relative amount of T helper cells, where the transcriptomic variance explained up to 88% of the phenotypic variance. As expected, the t^2 values were lower in those models considering also the genomic effect, except for carcass weight and % of phagocytic cells.

The heritability of the transcript-level effect on each trait (\tilde{h}_t^2), estimated in the GTCi model, is also shown in Table 2. This parameter varied widely across traits, taking values between 0.045 and 0.955. In general, the highest \tilde{h}_t^2 values were obtained for traits with negligible transcriptomic effects, such as carcass weight or cortisol concentrations, whereas traits with high transcriptomic contribution, such as lymphocytes count or $\gamma\delta$ T cells, showed \tilde{h}_t^2 bellow 0.1. The one notable exception to this trend was HP concentration, for which both t^2 and \tilde{h}_t^2 estimates took values above 0.8, but also T helper cells that showed medium \tilde{h}_t^2 having relevant transcriptomic contribution.

Models fit of immunity traits

The improvement in model fit from considering either transcriptomic or genomic effects in the model was evaluated by a likelihood ratio test comparing models that incorporate both effects (GT, GTC, GTCi models) against either G or T models. Additionally, both G and T models were compared to a fixed effects model (i.e. without random effects). The statistics from these model comparisons are presented in Table 3. Both G and T models presented a highly significant (P -value $< 10^{-5}$) increase in the likelihood regarding a fixed model, thus confirming these omics effects on

all the analysed traits. Models considering both genomic and transcriptomic effects provided a better fit than the G model for all traits, except for those with the lowest t^2 estimates: cortisol concentration in both serum and hair, carcass weight, and in some comparisons, the phagocytic uptake. Incorporating genomic effects into models with transcriptomic effects (the comparison between T and GT models) also improved the model fit for certain traits; however, this result was less consistent across traits and model comparisons. The most significant fit improvement derived from incorporating genomic effects into a model with transcriptomics was observed for those traits with high heritability, such as plasma immunoglobulin G concentration and carcass weight. Conversely, the fit for HP concentration, phagocytic traits, monocytes count, or lymphocytes count did not improve with the addition of genomic effects to a model with transcriptomics.

Predicting immunity traits from multiomic data

The accuracy (obtained by cross-validation) of phenotypic prediction of immunity and carcass traits with the different models considering omics data is reported in Table 4 and Fig. S1. With the G model, prediction accuracies were below 0.4 for all traits. The highest prediction accuracies were for $\gamma\delta$ T cells (0.387), followed by plasma immunoglobulin G and M concentrations (0.368 and 0.341), carcass weight (0.330) and T helper cells amount (0.329). As expected, prediction accuracy from the G model was highly correlated (0.972) with the heritability estimate of the trait, so traits with the lowest heritabilities (% of phagocytic cells and monocytes count) presented the lowest accuracies. The model considering transcriptomic effects (T) presented prediction accuracies correlating with the t^2 (0.872). This accuracy was above

Table 3

Significance (*P*-value) of the likelihood ratio test (LRT) between models incorporating both genomic and transcriptomic effects vs models with either genomic or transcriptomic effects, for different pig immunity-related and carcass traits. Models: genomic model (G), transcriptomic model (T), genomic and transcriptomic as independent effects (GT), transcriptomics conditioned to genomics on the basis of either the heritability of the trait (GTC) or the heritability of transcriptomic effects (GTCi).

Traits	LRT vs fixed model		LRT vs GBLUP			LRT vs TBLUP	
	G model	T model	GT model	GTC model	GTCi model	GT model	
Immunoglobulin M in plasma (mg/mL)	$<1 \times 10^{-5}$	$<1 \times 10^{-5}$	7.1×10^{-3}	8.8×10^{-3}	3.1×10^{-3}	2.2×10^{-3}	
Immunoglobulin G in plasma (mg/mL)	$<1 \times 10^{-5}$	$<1 \times 10^{-5}$	1.7×10^{-2}	2.7×10^{-2}	1.8×10^{-2}	7.4×10^{-5}	
Haptoglobin in serum (mg/mL)	$<1 \times 10^{-5}$	$<1 \times 10^{-5}$	$<1 \times 10^{-5}$	$<1 \times 10^{-5}$	$<1 \times 10^{-5}$	1.1×10^{-1}	
C-reactive protein in serum (μ g/mL)	$<1 \times 10^{-5}$	$<1 \times 10^{-5}$	$<1 \times 10^{-5}$	$<1 \times 10^{-5}$	$<1 \times 10^{-5}$	1.7×10^{-2}	
Phagocytic cells (%)	$<1 \times 10^{-5}$	$<1 \times 10^{-5}$	$<1 \times 10^{-5}$	$<1 \times 10^{-5}$	$<1 \times 10^{-5}$	1.4×10^{-1}	
Phagocytic uptake (FITC)	$<1 \times 10^{-5}$	$<1 \times 10^{-5}$	1.9×10^{-3}	2.3×10^{-3}	5.0×10^{-1}	2.2×10^{-1}	
Leukocytes count (n/ μ L)	$<1 \times 10^{-5}$	$<1 \times 10^{-5}$	$<1 \times 10^{-5}$	$<1 \times 10^{-5}$	$<1 \times 10^{-5}$	1.7×10^{-2}	
Lymphocytes count (n/ μ L)	$<1 \times 10^{-5}$	$<1 \times 10^{-5}$	$<1 \times 10^{-5}$	$<1 \times 10^{-5}$	$<1 \times 10^{-5}$	1.2×10^{-1}	
Monocytes count (n/ μ L)	$<1 \times 10^{-5}$	$<1 \times 10^{-5}$	1.6×10^{-4}	5.5×10^{-4}	2.6×10^{-2}	7.0×10^{-2}	
T helper cells (% of PBMCs)	$<1 \times 10^{-5}$	$<1 \times 10^{-5}$	1.2×10^{-1}	1.2×10^{-1}	6.0×10^{-2}	4.7×10^{-2}	
$\gamma\delta$ T cells (% of PBMCs)	$<1 \times 10^{-5}$	$<1 \times 10^{-5}$	$<1 \times 10^{-5}$	$<1 \times 10^{-5}$	$<1 \times 10^{-5}$	3.7×10^{-3}	
Cortisol in plasma (nM)	$<1 \times 10^{-5}$	$<1 \times 10^{-5}$	2.9×10^{-1}	3.1×10^{-1}	2.5×10^{-1}	2.7×10^{-3}	
Cortisol in hair (pg/mg)	$<1 \times 10^{-5}$	$<1 \times 10^{-5}$	$<1 \times 10^{-5}$	$<1 \times 10^{-5}$	$<1 \times 10^{-5}$	3.0×10^{-2}	
Carcass weight (kg)	$<1 \times 10^{-5}$	$<1 \times 10^{-5}$	2.9×10^{-1}	2.3×10^{-1}	1.3×10^{-1}	$<1 \times 10^{-5}$	

Abbreviations: FITC = Fluorescein emission; PBMC = Peripheral blood mononuclear cells.

Table 4

Accuracy (mean and 95% confidence interval) of phenotype prediction for pig immunity-related and carcass traits with different models incorporating omics information: genomic model (G), transcriptomic model (T), genomic and transcriptomic as independent effects (GT), transcriptomics conditioned to genomics on the basis of either the heritability of the trait (GTC) or the heritability of transcriptomic effects (GTCi), and multiomic model (M).

Traits	G model		T model		GT model		GTC model		GTCi model		M model	
	Value	CI	Value	CI	Value	CI	Value	CI	Value	CI	Value	CI
Immunoglobulin M in plasma (mg/mL)	0.341	[0.065,0.631]	0.400	[0.081,0.653]	0.410	[0.030,0.685]	0.345	[0.053,0.622]	0.371	[0.16,0.536]	0.427	[0.047,0.699]
Immunoglobulin G in plasma (mg/mL)	0.368	[-0.024,0.685]	0.292	[-0.064,0.556]	0.377	[-0.014,0.673]	0.372	[-0.040,0.689]	0.366	[0.109,0.579]	0.390	[0.004,0.674]
Haptoglobin in serum (mg/mL)	0.162	[-0.238,0.474]	0.561	[0.218,0.786]	0.552	[0.222,0.758]	0.188	[-0.201,0.505]	0.455	[0.269,0.607]	0.559	[0.228,0.767]
C-reactive protein in serum (μ g/mL)	0.165	[-0.168,0.509]	0.406	[0.081,0.668]	0.410	[0.045,0.669]	0.181	[-0.154,0.513]	0.390	[0.187,0.564]	0.422	[0.077,0.675]
Phagocytic cells (%)	0.051	[-0.318,0.353]	0.568	[0.189,0.822]	0.570	[0.205,0.812]	0.133	[-0.208,0.470]	0.550	[0.329,0.750]	0.573	[0.204,0.818]
Phagocytic uptake (FITC)	0.100	[-0.264,0.419]	0.198	[-0.228,0.589]	0.182	[-0.217,0.541]	0.046	[-0.312,0.357]	0.097	[-0.163,0.332]	0.208	[-0.184,0.569]
Leukocytes count (n/ μ L)	0.204	[-0.145,0.515]	0.595	[0.308,0.798]	0.600	[0.324,0.796]	0.203	[-0.158,0.516]	0.610	[0.426,0.734]	0.604	[0.327,0.800]
Lymphocytes count (n/ μ L)	0.236	[-0.132,0.538]	0.594	[0.308,0.809]	0.602	[0.318,0.817]	0.268	[-0.087,0.565]	0.566	[0.381,0.72]	0.606	[0.326,0.819]
Monocytes count (n/ μ L)	0.064	[-0.267,0.421]	0.512	[0.160,0.775]	0.509	[0.161,0.770]	0.064	[-0.282,0.411]	0.478	[0.235,0.675]	0.517	[0.175,0.770]
T helper cells (% of PBMCs)	0.329	[-0.074,0.655]	0.457	[0.097,0.743]	0.427	[0.066,0.726]	0.309	[-0.065,0.649]	0.287	[0.007,0.519]	0.464	[0.102,0.743]
$\gamma\delta$ T cells (% of PBMCs)	0.387	[0.022,0.659]	0.596	[0.249,0.810]	0.606	[0.275,0.814]	0.427	[0.121,0.674]	0.617	[0.441,0.761]	0.610	[0.284,0.816]
Cortisol in plasma (nM)	0.135	[-0.268,0.508]	0.149	[-0.182,0.442]	0.150	[-0.235,0.512]	0.136	[-0.257,0.512]	0.256	[0.038,0.448]	0.177	[-0.205,0.531]
Cortisol in hair (pg/mg)	0.273	[-0.123,0.594]	0.190	[-0.147,0.485]	0.259	[-0.104,0.579]	0.332	[-0.033,0.619]	0.128	[-0.117,0.355]	0.277	[-0.079,0.577]
Carcass weight (kg)	0.330	[-0.029,0.622]	-0.133	[-0.424,0.085]	0.323	[-0.023,0.625]	0.285	[-0.093,0.595]	0.228	[0.046,0.424]	0.335	[-0.014,0.626]

Abbreviations: FITC = Fluorescein emission; PBMC = Peripheral blood mononuclear cells.

0.50 for traits with high t^2 : different leukocyte counts, proportion of $\gamma\delta$ T cells, % of phagocytic cells and HP concentration in plasma. These same traits were also the best predicted (accuracy from 0.51 to 0.61) under the GT model.

Among models fitting both genomic and transcriptomic effects, the GTC model performed similarly to the G model in terms of prediction accuracy. The highest accuracy was observed for traits with high heritability, being $\gamma\delta$ T cells the trait best predicted under the GTC model (mean accuracy of 0.43), followed by plasma immunoglobulin G and M concentrations (0.37 and 0.35); the lowest accuracy (below 0.06) was for phagocytic uptake and monocyte count. Models including genomic and transcriptomic effects (GT, GTCi and M models) yielded accuracies above 0.5 for those traits with high transcriptomic contribution, such as $\gamma\delta$ T cells (accuracy 0.61), different leukocyte counts (from 0.48 to 0.61), HP concentration (0.56) and % of phagocytic cells (0.55 and 0.57). Hardly any differences were observed between the prediction accuracies provided by GTCi and M models, but for T helper cells.

To increase the discriminatory power when comparing accuracies between models, within-trait differences in prediction accuracy across cross-validation iterations were also calculated and are shown in Fig. 2 and presented in Table S2. All models considering the two omics effects but GTC model (i.e. GT, GTCi and M models) showed better prediction accuracy than the G model for different leukocyte and lymphocyte counts. Predictions from GTCi in general were the most accurate but accuracies were similar to the M model. The GTCi model also performed better than the G model in predicting serum HP concentrations and was suggestive to better predict the concentration of CRP, $\gamma\delta$ T cells and % of phagocytic cells, while surpassing GTC for monocyte count. Conversely, when comparing the four two-omics models (GT, GTC, GTCi and M models) with the transcriptomic model, no relevant increase in the prediction ability of the model was detected for any of the analysed traits but carcass weight. What is more, the GTC underperformed compared to the T model in predicting leukocyte count and serum HP concentration.

Breeding value accuracy

The accuracy of the predicted breeding values for immunity and carcass traits under the models including additive genetic effects (i.e. GT, GTC and GTCi models) is presented in Table 5. The breeding value accuracy varied greatly between traits, but not so much across models (within trait). Across traits, the breeding value accuracy was closely related to the estimated heritabilities. Accordingly, the highest accuracies of genetic evaluation were obtained for plasma immunoglobulin G and M concentration and the amount of $\gamma\delta$ T cells (accuracies from 0.32 to 0.43). Carcass weight also maintained relatively high genetic prediction accuracy across models (from 0.27 to 0.29). Conversely, the % of phagocytic cells and monocytes count presented the lowest breeding value accuracies across all models (from 0.05 to 0.13).

Between-model differences in the accuracy of genetic evaluation for the different traits are presented in Fig. S2. It can be observed that GTC offered the best genetic evaluation in terms of breeding value accuracy for several immunity traits, particularly for $\gamma\delta$ T cells, % of phagocytic cells, immunoglobulin concentrations (both G and M), and lymphocyte count. For other traits, such as HP and CRP concentrations, and leukocytes and monocytes count, the highest breeding value accuracy was obtained with the GTCi model.

Discussion

The inclusion of immunity traits into pig breeding programmes is a promising strategy for improving animal robustness and disease resistance. In the present study, we evaluated the potential to include transcriptomic information into genomic evaluation models to better predict immunity traits in pigs. To achieve our objective, we tested different mixed-modelling strategies across 14 traits, including immunity traits such as immunoglobulins (M and G), HP and CRP concentrations, % of phagocytic cells and uptake, leukocytes, monocytes and lymphocytes counts, proportions of T helper cells and $\gamma\delta$ T cells, as well as welfare and production traits such as carcass weight and cortisol concentration in plasma and hair.

Medium to high heritabilities were obtained for the analysed traits across models considering the additive genetic effect with a genomic relationship matrix. According to these estimates, T cell subpopulations' relative abundance and immunoglobulin G concentration were the most heritable traits, while % of phagocytic cells and monocyte count were the lowest. These heritability estimates were similar if not a bit lower to those previously obtained in the same population (Jové-Juncà et al., 2024; Ballester et al., 2020, 2023) with a pedigree-based animal model, and also similar to the ones described for these traits in other populations (Flori et al., 2011; Clapperton et al., 2008, 2009; Henryon et al., 2006; Edfors-Lilja et al., 1994). When transcriptomic data were considered in the model, the estimated heritability decreased for most of the traits analysed but those with low heritability, as previously reported by Morgante et al. (2020) and Wade et al. (2022) for complex traits like starvation resistance and pathogen tolerance in reference species such as *Drosophila melanogaster* and *Populus nigra*. In our study, the decrease regarding the heritability estimated in the G model was generally lower when the covariance between genomic and transcriptomic effects was removed in the model (i.e. GTC and GTCi) than when both genomic and transcriptomic effects were considered as independent (i.e. GT). This is consistent with the rationale behind GTC and GTCi, in which the fraction of the genetic effect captured by the transcriptome was subtracted from the model, thereby simplifying the estimation of genetic effects from the genomic relationship matrix. It is, however, impor-

tant mentioning that the confidence intervals of heritability estimates of different models overlapped, so these results were not totally conclusive.

The estimated proportion of phenotypic variance explained by the blood transcriptome varied considerably among traits but was generally larger than the estimated heritability, exceeding 50% of the total variance for 10 out of the 14 analysed traits. It should be noted that the prediction accuracy obtained in the model, including only transcriptomic effects (T), was highly correlated to the proportion of phenotypic variance explained by the blood transcriptome. This way, for those traits with higher t^2 estimates, the blood transcriptome allowed much better phenotypic prediction than the genomic model, suggesting that the transcriptome acts as an "intermediate phenotype" that captures part of the genetic variation of the traits.

The traits with the highest transcriptomic contribution were the abundance of T helper cells and HP concentration, followed by leukocyte count and $\gamma\delta$ T cells, showing values similar to those reported by Morgante et al. (2020) for starvation resistance in *Drosophila melanogaster*. All the traits are known to be functionally related to immunity and immunocompetence (Ballester et al., 2020, 2023; Holtmeier and Kabelitz, 2005; Mair et al., 2014; Noelle and Snow, 1992). Leukocyte count has been associated with survivability after PRRSV infection (Tarrés et al., 2024), and specific leukocyte subsets, such as T helper and $\gamma\delta$ T cells, are well-known markers of immune activation following infection or vaccination (Pedrera et al., 2024; Schmidt et al., 2021) and have also been linked to disease resistance in pigs (Le Page et al., 2022; Tarrés et al., 2024). Additionally, serum HP concentration has shown links with gut symbiotic microbiota and may play a role in the occurrence of opportunistic pathogens (Ramayo-Caldas et al., 2021).

On the opposite side, the cortisol concentration in hair and the carcass weight showed scarce contribution of the blood transcriptome. The transcriptome is highly dependent on both tissue and sampling time (Perez et al., 2022; Azodi et al., 2019; Guo et al., 2016). As such, it is plausible that cortisol concentration in hair was lowly associated with the blood transcriptome, and the panel of gene-expression levels obtained at 60 days of age, far before the age of slaughter at 180 days, was poorly related to carcass weight. The transcriptome predictive value for these traits would be expected to improve if the expression panel were analysed at a time closer to the phenotype measure and/or from tissues more functionally related, such as the adrenal gland or liver for cortisol concentration, and muscle, liver, or adipose tissue for carcass weight.

In line with the estimated transcriptomic effects, the inclusion of transcriptomic data in the model allowed capturing a higher proportion of phenotypic variance than the genomic prediction model for the vast majority of immunity traits. This is also concordant with results obtained in previous studies (Haas et al., 2025; Perez et al., 2022) for metabolic and production traits in mice and quails. Conversely, the addition of genomic data to models already considering transcriptomic information provided a less consistent improvement of fit, only notable in the traits with the highest heritability estimates. This reinforces the idea proposed by Michel et al. (2021) that genetic effects may be almost fully represented by the transcriptomic profile. Among the analysed immunity traits, nearly all genetic variance of T helper cells and $\gamma\delta$ T cells, leukocytes, and HP concentration appeared to be captured by the transcriptomic component.

Among models including both genomic and transcriptomic effects, the GTCi model captured the largest proportion of phenotypic variance for the majority of analysed traits, while the model considering genomic and transcriptomic effects as independent (GT) captured the least. As indicated by Haas et al. (2025), correct-

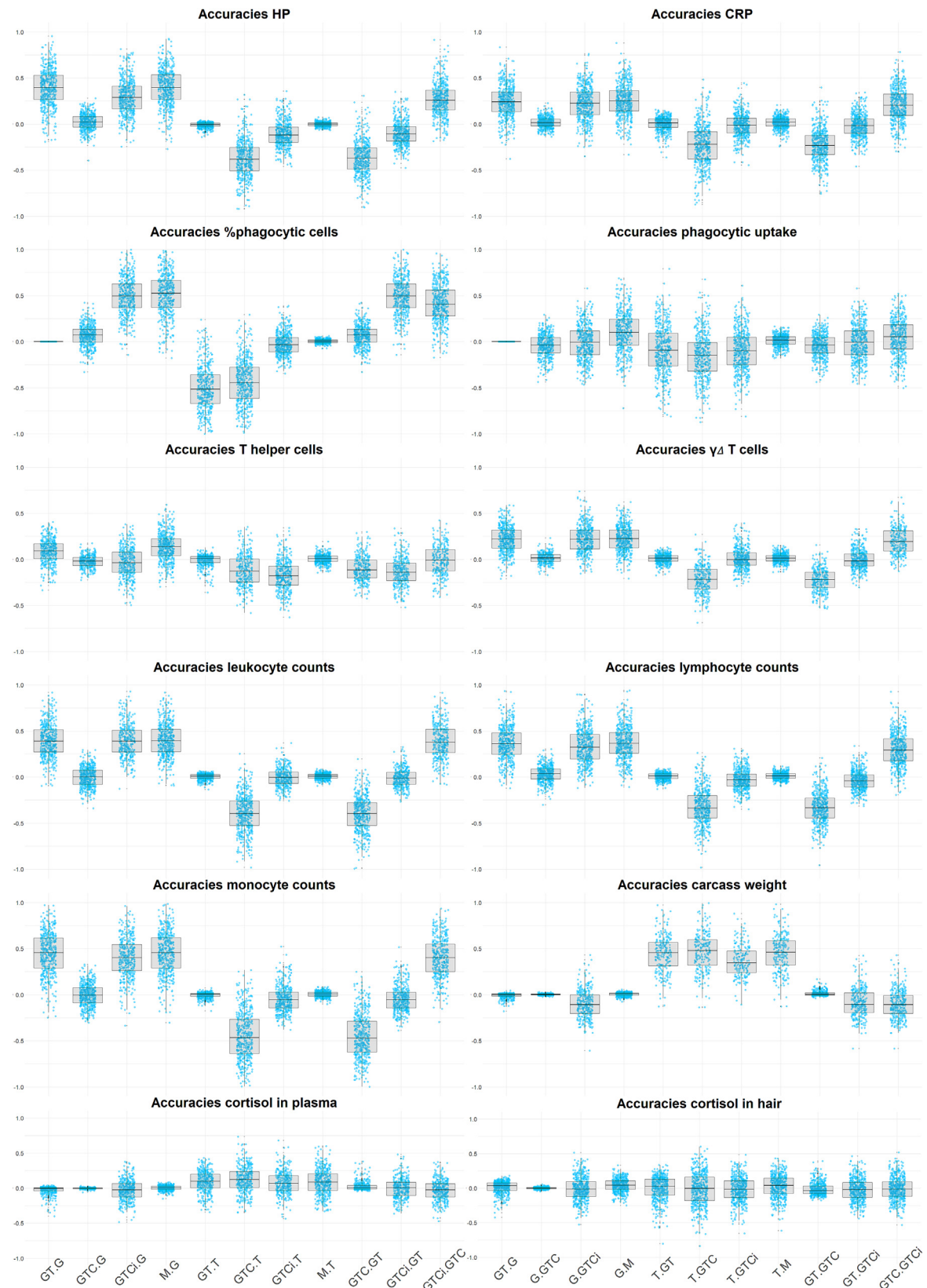


Fig. 2. Boxplots depicting differences in accuracy of porcine immunity phenotypes prediction between different models: genomic (G), transcriptomic (T), genomic and transcriptomic as independent effects (GT), transcriptomics conditioned to genomics on the basis of either the heritability of the trait (GTC) or the heritability of transcriptomic effects (GTCi), and multiomic (M) models. CRP and HP stand for C-reactive protein and haptoglobin concentrations in serum, respectively.

Table 5

Accuracy (mean and 95% confidence interval) of breeding value prediction for pig immunity-related and carcass traits with different models incorporating omics information: genomic model (G), genomic and transcriptomic model (GT), genomic and transcriptomic as independent effects (GTC), transcriptomics conditioned to genomics on the basis of either the heritability of the trait (GTCi) or the heritability of transcriptomic effects (GTCi).

Traits	G model		GT model		GTC model		GTCi model	
	Value	CI	Value	CI	Value	CI	Value	CI
Immunoglobulin M in plasma (mg/mL)	0.341	[-0.065,0.631]	0.341	[-0.057,0.612]	0.345	[-0.053,0.622]	0.327	[0.113,0.508]
Immunoglobulin G in plasma (mg/mL)	0.368	[-0.024,0.685]	0.367	[-0.031,0.684]	0.372	[-0.040,0.689]	0.360	[0.083,0.581]
Haptoglobin in serum (mg/mL)	0.162	[-0.238,0.474]	0.150	[-0.258,0.504]	0.188	[-0.201,0.505]	0.209	[-0.016,0.417]
C-reactive protein in serum (µg/mL)	0.165	[-0.168,0.509]	0.178	[-0.155,0.499]	0.181	[-0.154,0.513]	0.182	[-0.061,0.396]
Phagocytic cells (%)	0.051	[-0.318,0.353]	0.051	[-0.318,0.353]	0.133	[-0.208,0.470]	0.096	[-0.146,0.345]
Phagocytic uptake (FITC) ¹	0.100	[-0.264,0.419]	0.100	[-0.264,0.419]	0.046	[-0.312,0.357]	0.049	[-0.200,0.286]
Leukocytes count (n/µL)	0.204	[-0.145,0.515]	0.171	[-0.194,0.475]	0.203	[-0.158,0.516]	0.207	[-0.046,0.421]
Lymphocytes count (n/µL)	0.236	[-0.132,0.538]	0.232	[-0.126,0.540]	0.268	[-0.087,0.565]	0.203	[-0.073,0.436]
Monocytes count (n/µL)	0.064	[-0.267,0.421]	0.051	[-0.294,0.393]	0.064	[-0.282,0.411]	0.155	[-0.076,0.362]
T helper cells (% of PBMCs) ¹	0.329	[-0.074,0.655]	0.287	[-0.115,0.638]	0.309	[-0.065,0.649]	0.250	[-0.008,0.493]
γδ T cells (% of PBMCs) ¹	0.387	[0.022,0.659]	0.351	[0.004,0.642]	0.427	[0.121,0.674]	0.380	[0.179,0.589]
Cortisol in plasma (nM)	0.273	[-0.123,0.594]	0.282	[-0.093,0.590]	0.285	[-0.093,0.595]	0.271	[0.037,0.468]
Cortisol in hair (pg/mg)	0.135	[-0.268,0.508]	0.135	[-0.258,0.509]	0.136	[-0.257,0.512]	0.115	[-0.145,0.346]
Carcass weight (kg)	0.330	[-0.029,0.622]	0.334	[-0.024,0.621]	0.332	[-0.033,0.619]	0.248	[0.049,0.450]

Abbreviations: FITC = Fluorescein emission; PBMC = Peripheral blood mononuclear cells.

ing for redundant information between the genetic and transcriptomic effects generally results in a lower residual variance. Our results also suggest that the GTCi modification proposed by [Haas et al. \(2025\)](#) addresses the overlap between genomic and transcriptomic information more effectively than the GTC and M models.

Both GTC and GTCi models aimed to remove the covariation between genomic and transcriptomic effects, but the GTCi model corrected on the basis of the estimated heritability of the transcriptomic effects, rather than on the heritability of the trait, as in the GTC. In fact, the heritability of the transcriptomic effects on the phenotypes (\tilde{h}_t^2) differed notably from the heritability of the trait, while it tended to be larger in those traits with low variance of transcriptomic effects. Among immunity traits with relevant transcriptomic contribution, the serum HP concentration showed by far the highest heritability of transcriptomic effects, indicating that most of the transcriptomic effects variance on this trait was explained by additive genetic effects. Conversely, except for T helper cell abundance and immunoglobulin M concentration that showed medium \tilde{h}_t^2 , the transcriptomic effects on the rest of immunity traits were mainly modulated by other sources of variability, such as environmental or physiological variability, and had a negligible heritable component.

The M model also tried to correct for redundant information, introducing a ratio (\tilde{r}), between the impact of genomic and transcriptomic effects. The amount of variance captured by the M model was, however, lower than that captured by GTCi. Despite weighting the genomic and transcriptomic effects in the multi-omics relationship matrix, the M model captured the same proportion of phenotypic variance than considering both effects as independent (GT), as in fact, the variance of multiomic effects of M closely corresponded to the weighted sum of transcriptomic and transcriptomic variances in the GT.

The capability of the studied models to predict the immunity traits was analysed in terms of their phenotypic prediction accuracy obtained by cross-validation, observing that in general, the G model had the lowest accuracy compared to the rest of models, while GTCi and M models tend to have the highest ones for most of the traits. In general, GTCi and M showed similar predictive performance across traits, suggesting certain statistical equivalence between the two iterative procedures to approach the relationship between genomic and transcriptomic effects on each trait. While the limited sample size led to wide and generally overlapped confidence intervals for these accuracies, significant

differences were observed when applying [Schrauf et al. \(2021\)](#) methodology, i.e. selecting the same test population for all models at each iteration of the cross-validation. This procedure successfully eliminated the variability generated by the random selection of the test population and allowed confirming the improvement in phenotypic prediction derived from including transcriptomic information in the case of white cells (leukocytes, monocytes and lymphocytes) counts and the proportion of phagocytic cells. In all cases, GTCi significantly outperformed conventional GBLUP, and also GTCBLUP for leukocytes, whereas M outperformed G only for leukocytes and lymphocytes. Differences between GTCi and M accuracies were not significant. This way, the better fit of models incorporating transcriptomic data did not always translate into better phenotypic prediction; probably, a larger sample size would allow observing larger significant differences across models. The high accuracy of phenotype predictions when considering transcriptomic information would suggest that environmental effects were partially captured by the transcriptomic effect. Similar increases in accuracy were reported by [Haas et al. \(2025\)](#) in their study for P and Ca utilisation, BW gain, feed intake, and feed conversion ratio in quails. However, these authors also observed a greater accuracy of GTC when compared with the G model. As previously reported by [Perez et al. \(2022\)](#), the increase in accuracy derived from incorporating transcriptomic effects was dependent on the transcriptomic effect contribution to phenotypic variation (i.e. positively correlated with t^2). Among the analysed immunity traits, a particular increase in accuracy was observed for leukocyte and lymphocyte counts, $\gamma\delta$ T cells and % of phagocytic cells, whereas the prediction accuracy did not increase regarding G model levels for traits lowly associated with transcriptomic effects such as cortisol concentrations.

Finally, the accuracy of genetic evaluation was also assessed, but no significant differences across models for the accuracy of predicted breeding value were reported. Only a suggestive superiority of the accuracy obtained in the GTC for HP and CRP concentrations, % of phagocytic cells, lymphocytes count and $\gamma\delta$ T cells, and GTCi for monocytes and leukocytes counts and HP and CRP concentrations was observed. These results are in agreement with those reported by [Perez et al. \(2022\)](#) in bone mineral density, BW, fat percentage and circulating cortisol and triglycerides, who found better genomic prediction with GTC than with G models. In any case, the wide confidence intervals prevented us from drawing definitive conclusions in this regard.

Within the model, differences across immunity traits regarding the accuracy of genetic evaluation followed the same pattern than heritability estimates. This way, traits belonging to adaptive immune processes, such as immunoglobulin concentrations or T helper cells proportion, presented a high accuracy of genetic evaluation, while traits belonging to innate immunity processes (e.g. traits related to phagocytosis or monocytes count) had a low accuracy of predicted breeding values. The most accurate genetic evaluation was obtained for the proportion of $\gamma\delta$ T cells, which are involved in both types of immunity (innate and adaptive). The cortisol concentrations, not directly involved in immunity but acting as stress indicators, presented disparate accuracies and \hat{h}^2 , suggesting a higher environmental effect on the measure of chronic stress (cortisol in hair) than on the acute stress (cortisol in plasma). As a whole, genetic evaluation accuracies endorse the potential success of a breeding programme to improve robustness based on adaptive immunity traits, and particularly on the abundance of $\gamma\delta$ T cells subpopulation, a trait previously remarked as a potential selection criteria for its high heritability (Ballester et al., 2020, 2023) and links to production performance (Jové-Juncà et al., 2024; Meng et al., 2021). The present study has gone further by testing the potential of transcriptomic information to improve the prediction of these immunity traits using different modelling strategies. However, the limited sample size did not allow to be conclusive regarding the accuracy of the genetic evaluation when considering transcriptomic information in the model. Moreover, the present study has focused on piglets' blood transcriptome and immunity status during the transitional stage (60 days of age), in which animals are exposed to several stressors and robustness is particularly relevant, but transcriptomic profiles are known to vary across time and tissues (Bryois et al., 2017; Teng et al., 2022). Future research should validate these findings in larger sample sizes, different populations and other physiological stages. Also, comparing transcriptomic contribution from other tissues functionally related to immunity, such as spleen or lymph nodes, would be worthy. Finally, the design of targeted panels of functionally relevant transcripts that may capture most of the transcriptomic contribution to immunity phenotypes, as reported by Haas et al. (2025) for productive traits in quails, remains as an interesting approach for a more affordable prediction of immunity profiles from transcriptomic data.

In conclusion, the addition of transcriptomic information to genetic evaluation models improved model fit and phenotypic prediction of pigs' immunity traits, particularly for traits with a high transcriptomic contribution, such as HP concentration, leukocyte counts, $\gamma\delta$ T cells and T helper cells abundances. Furthermore, the transcriptome could be used to predict traits that are strongly influenced by environmental factors and are difficult to measure directly, such as immune cell subpopulations or the phagocytic index. The models that corrected for overlap among omics data layers performed best for most immunity traits, particularly when adjusting by the heritability of the transcriptomic effect and when dealing with traits with a strong transcriptomic influence. Based on the results presented in this study, we conclude that the genomic prediction of immunity traits is feasible and can be substantially improved by the inclusion and proper modelling of transcriptomic data.

Supplementary material

Supplementary Material for this article (<https://doi.org/10.1016/j.animal.2025.101742>) can be found at the foot of the online page, in the Appendix section.

Ethics approval

All experimental procedures involving living animals that were performed in this study were designed in compliance with the

Spanish Policy of Animal Protection RD 53/2013 under the European Union Directive 2010/63/EU regarding the use of animals in experimentation. The protocols were then reviewed by the Ethical Committee of the Institut de Recerca i Tecnologia Agroalimentàries (IRTA) and subsequently approved.

Data and model availability statement

The raw sequence data used in this study have been deposited in the SRA repository with the Bioproject accession code PRJNA1267984 and can be found in the link: <https://www.ncbi.nlm.nih.gov/bioproject/PRJNA1267984> after 2026-11-20. Other data used in this study, such as phenotypes, are available from the authors upon request.

Declaration of generative AI and AI-assisted technologies in the writing process

During the preparation of this work the author(s) did not use any AI and AI-assisted technologies.

Author ORCIDs

T. Jové-Juncà: <https://orcid.org/0000-0002-6436-3279>.
V.P. Haas: <https://orcid.org/0000-0002-9651-1205>.
M. Calus: <https://orcid.org/0000-0002-3213-704X>.
M. Ballester: <https://orcid.org/0000-0002-5413-4640>.
R. Quintanilla: <https://orcid.org/0000-0003-3274-3434>.

CRedit authorship contribution statement

T. Jové-Juncà: Writing – original draft, Visualisation, Software, Investigation, Formal analysis, Data curation. **V.P. Haas:** Writing – review & editing, Resources, Methodology. **M.P.L. Calus:** Writing – review & editing, Supervision, Resources, Methodology. **M. Ballester:** Writing – review & editing, Supervision, Resources, Project administration, Investigation, Funding acquisition, Conceptualisation. **R. Quintanilla:** Writing – review & editing, Supervision, Resources, Investigation, Funding acquisition, Conceptualisation.

Declaration of interest

The authors declare that they have no competing interests.

Acknowledgements

Authors acknowledge Selecció Batallé S.A. for providing the animal material and for their close collaboration in farm and slaughterhouse.

Financial support statement

This study was funded by grants PID2020-112677RB-C21 and PID2023-148961OB-C21 awarded by MCIN/AEI/10.13039/501100011033. Jové-Juncà, T. was supported by an IRTA fellowship (CPI1221).

References

Azodi, C.B., Bolger, E., McCarren, A., Roantree, M., de los Campos, G., Shiu, S.H., 2019. Benchmarking parametric and machine learning models for genomic prediction of complex traits. *G3 Genes|genomes|genetics* 9, 3691–3702. <https://doi.org/10.1534/G3.119.400498>.
Ballester, M., Ramayo-Caldas, Y., González-Rodríguez, O., Pascual, M., Reixach, J., Díaz, M., Blanc, F., López-Serrano, S., Tibau, J., Quintanilla, R., 2020. Genetic

parameters and associated genomic regions for global immunocompetence and other health-related traits in pigs. *Scientific Reports* 10, 18462. <https://doi.org/10.1038/S41598-020-75417-7>.

Ballester, M., Jové-Juncà, T., Pascual, A., López-Serrano, S., Crespo-Piazuelo, D., Hernández-Banqué, C., González-Rodríguez, O., Ramayo-Caldas, Y., Quintanilla, R., 2023. Genetic architecture of innate and adaptive immune cells in pigs. *Frontiers in Immunology* 14, 1058346. <https://doi.org/10.3389/FIMMU.2023.1058346>.

Browning, B.L., Zhou, Y., Browning, S.R., 2018. A one-penny imputed genome from next-generation reference panels. *The American Journal of Human Genetics* 103, 338–348. <https://doi.org/10.1016/j.ajhg.2018.07.015>.

Bryois, J., Buil, A., Ferreira, P.G., Panousis, N.I., Brown, A.A., Viñuela, A., Planchon, A., Bielser, D., Small, K., Spector, T., Dermitzakis, E.T., 2017. Time-dependent genetic effects on gene expression implicate aging processes. *Genome Research* 27, 545–552. <https://doi.org/10.1101/GR.207688.116>.

Butler, D.G., Cullis, B.R., Gilmour, A.R., Gogel, B.J., Thompson, R., 2023. ASReml-R reference manual version 4.2. National Institute for Applied Statistics and Research. VSN International Ltd, Hemel Hempstead, UK.

Cheung, V.G., Conlin, L.K., Weber, T.M., Arcaro, M., Jen, K.Y., Morley, M., Spielman, R. S., 2003. Natural variation in human gene expression assessed in lymphoblastoid cells. *Nature Genetics* 33, 422–425. <https://doi.org/10.1038/NG1094>.

Christensen, O.F., Börner, V., Varona, L., Legarra, A., 2021. Genetic evaluation including intermediate omics features. *Genetics* 219, iyab130. <https://doi.org/10.1093/GENETICS/IYAB130>.

Clapperton, M., Glass, E.J., Bishop, S.C., 2008. Pig peripheral blood mononuclear leucocyte subsets are heritable and genetically correlated with performance. *Animal* 2, 1575–1584. <https://doi.org/10.1017/S1751731108002929>.

Clapperton, M., Diack, A.B., Matika, O., Glass, E.J., Gladney, C.D., Mellencamp, M.A., Hoste, A., Bishop, S.C., 2009. Traits associated with innate and adaptive immunity in pigs: Heritability and associations with performance under different health status conditions. *Genetics Selection Evolution* 41, 1–11. <https://doi.org/10.1186/1297-9686-41-54/TABLES/6>.

DOBIN, A., DAVIS, C.A., SCHLESINGER, F., DRENKOW, J., ZALESKI, C., JHA, S., BATUT, P., CHAISSON, M., GINGERAS, T.R., 2013. STAR: ultrafast universal RNA-seq aligner. *Bioinformatics (oxford, England)* 29, 15–21. <https://doi.org/10.1093/BIOINFORMATICS/BTS635>.

Edfors-Lilja, I., Watström, E., Magnusson, U., Fossum, C., 1994. Genetic variation in parameters reflecting immune competence of swine. *Veterinary Immunology and Immunopathology* 40, 1–16. [https://doi.org/10.1016/0165-2427\(94\)90011-6](https://doi.org/10.1016/0165-2427(94)90011-6).

Flori, L., Gao, Y., Laloë, D., Lemonnier, G., Leplat, J.J., Teillaud, A., Cossalter, A.M., Laffitte, J., Pinton, P., de Vaureix, C., Bouffaoud, M., Mercat, M.J., Lefèvre, F., Oswald, I.P., Bidanel, J.P., Rogel-Gaillard, C., 2011. Immunity traits in pigs: substantial genetic variation and limited covariation. *PLoS One* 6, e22717. <https://doi.org/10.1371/JOURNAL.PONE.0022717>.

Guo, Z., Magwire, M.M., Basten, C.J., Xu, Z., Wang, D., 2016. Evaluation of the utility of gene expression and metabolic information for genomic prediction in maize. *TAG. Theoretical and applied genetics. Theoretische Und Angewandte Genetik* 129, 2413–2427. <https://doi.org/10.1007/S00122-016-2780-5>.

Haas, V., Wellman, R., Duenk, P., Oster, M., Ponsuksili, S., Bennewitz, J., Calus, M.P.L., 2025. Incorporating transcriptomic data into genomic prediction models to improve the prediction accuracy of phenotypes of efficiency traits. *Genetics Selection Evolution* 57, 59. <https://doi.org/10.1186/s12711-025-01008-7>.

Henryon, M., Heegaard, P.M.H., Nielsen, J., Berg, P., Juul-Madsen, H.R., 2006. Immunological traits have the potential to improve selection of pigs for resistance to clinical and subclinical disease. *Animal Science* 82, 596–606. <https://doi.org/10.1079/ASC200671>.

Holtmeier, W., Kabelitz, D., 2005. gammadelta T cells link innate and adaptive immune responses. *Chemical Immunology and Allergy* 86, 151–183. <https://doi.org/10.1159/000086659>.

Hothorn, T., Leisch, F., Zeileis, A., Hornik, K., 2005. The design and analysis of benchmark experiments. *Journal of Computational and Graphical Statistics* 14, 675–699. <https://doi.org/10.1198/106186005X59630>.

Hu, Z.L., Park, C.A., Reecy, J.M., 2022. Bringing the Animal QTLdb and CorrDB into the future: meeting new challenges and providing updated services. *Nucleic Acids Research* 50, D956–D961. <https://doi.org/10.1093/NAR/GKAB116>.

Jové-Juncà, T., Crespo-Piazuelo, D., González-Rodríguez, O., Pascual, M., Hernández-Banqué, C., Reixach, J., Quintanilla, R., Ballester, M., 2024. Genomic architecture of carcass and pork traits and their association with immune capacity. *Animal* 18, 101043. <https://doi.org/10.1016/J.ANIMAL.2023.101043>.

Knap, P.W., Bishop, S.C., 2000. Relationships between genetic change and infectious disease in domestic livestock. *BSAP Occasional Publication* 27, 65–80. <https://doi.org/10.1017/S1463981500040553>.

Le Page, L., Baldwin, C.L., Telfer, J.C., 2022. $\gamma\delta$ T cells in artiodactyls: focus on swine. *Developmental and Comparative Immunology* 128, 104334. <https://doi.org/10.1016/j.dci.2021.104334>.

Legarra, A., Christensen, O.F., 2022. Genomic evaluation methods to include intermediate correlated features such as high-throughput or omics phenotypes. *JDS Communications* 4, 55–60. <https://doi.org/10.33168/JDCS.2022-0276>.

Li, B., Dewey, C.N., 2011. RSEM: accurate transcript quantification from RNA-Seq data with or without a reference genome. *BMC Bioinformatics* 12, 1–16. <https://doi.org/10.1186/1471-2105-12-323/TABLES/6>.

Li, Z., Gao, N., Martini, J.W.R., Simianer, H., 2019. Integrating gene expression data into genomic prediction. *Frontiers in Genetics* 10, 430679. <https://doi.org/10.3389/FGENE.2019.00126/BIBTEX>.

Liang, M., An, B., Chang, T., Deng, T., Du, L., Li, K., Cao, S., Du, Y., Xu, L., Zhang, L., Gao, X., Li, J., Gao, H., 2022. Incorporating kernelized multi-omics data improves the accuracy of genomic prediction. *Journal of Animal Science and Biotechnology* 13, 103. <https://doi.org/10.1186/S40104-022-00756-6>.

Liu, J., Lang, K., Tan, S., Jie, W., Zhu, Y., Huang, S., Huang, W., 2022. A web-based database server using 43,710 public RNA-seq samples for the analysis of gene expression and alternative splicing in livestock animals. *BMC Genomics* 23, 706. <https://doi.org/10.1186/S12864-022-08881-2>.

Mair, K.H., Sedlak, C., Käser, T., Pasternak, A., Levast, B., Gerner, W., Saalmüller, A., Summerfield, A., Gerdtz, V., Wilson, H.L., Meurens, F., 2014. The porcine innate immune system: an update. *Developmental and Comparative Immunology* 45, 321–343. <https://doi.org/10.1016/J.DCI.2014.03.022>.

Meng, Z., Cao, G., Yang, Q., Yang, H., Hao, J., Yin, Z., 2021. Metabolic Control of $\gamma\delta$ T Cell Function. *Infectious Microbes and Diseases* 3, 142–148. <https://doi.org/10.1093/IM9.0000000000000054>.

Michel, S., Wagner, C., Nosenko, T., Steiner, B., Samad-Zamini, M., Buerstmayr, M., Mayer, K., Buerstmayr, H., 2021. Merging genomics and transcriptomics for predicting fusarium head blight resistance in wheat. *Genes* 12, 114. <https://doi.org/10.3390/GENES12010114>.

Misztal, I., Lourenco, D., Legarra, A., 2020. Current status of genomic evaluation. *Journal of Animal Science* 98, 4. <https://doi.org/10.1093/JAS/SKA101>.

Morgante, F., Huang, W., Sørensen, P., Maltecca, C., Mackay, T.F.C., 2020. Leveraging multiple layers of data to predict drosophila complex traits. *G3 (Bethesda, Md)* 10, 4599–4613. <https://doi.org/10.1534/G3.120.401847>.

Noelle, R., Snow, E.C., 1992. T helper cells. *Current Opinion in Immunology* 4, 333–337. [https://doi.org/10.1016/0952-7915\(92\)90085-S](https://doi.org/10.1016/0952-7915(92)90085-S).

Pedrera, M., Soler, A., Simón, A., Casado, N., Pérez, C., García-Casado, M.A., Fernández-Pacheco, P., Sánchez-Cordón, P.J., Arias, M., Gallardo, C., 2024. Characterization of the protective cellular immune response in pigs immunized intradermally with the live attenuated african swine fever virus (ASFV) Lv17/WB/Rie1. *Vaccines* 12, 443. <https://doi.org/10.3390/VACCINES12040443/S1>.

Perez, B.C., Bink, M.C.A.M., Svenson, K.L., Churchill, G.A., Calus, M.P.L., 2022. Adding gene transcripts into genomic prediction improves accuracy and reveals sampling time dependence. *G3 (Bethesda, Md)* 12, jkac258. <https://doi.org/10.1093/G3JOURNAL/JKAC258>.

Posit Team, P., 2025. RStudio: Integrated Development Environment for R. Posit Software, Boston, MA, USA.

Purcell, S., 2007. PLINK v1.90b342. Retrieved on 12/04/2023 from: <http://pngu.mgh.harvard.edu/purcell/plink/>.

Ramayo-Caldas, Y., Zingaretti, L.M., Pérez-Pascual, D., Alexandre, P.A., Reverter, A., Dalmau, A., Quintanilla, R., Ballester, M., 2021. Leveraging host-genetics and gut microbiota to determine immunocompetence in pigs. *Animal Microbiome* 3, 1–11. <https://doi.org/10.1186/S42523-021-00138-9/FIGURES/2>.

Robinson, M.D., McCarthy, D.J., Smyth, G.K., 2009. edgeR: a bioconductor package for differential expression analysis of digital gene expression data. *Bioinformatics* 26, 139–140. <https://doi.org/10.1093/BIOINFORMATICS/BTP161>.

Roth, K., Pröll-Cornelissen, M.J., Heuß, E.M., Dauben, C.M., Henne, H., Appel, A.K., Schellander, K., Tholen, E., Große-Brinkhaus, C., 2022. Genetic parameters of immune traits for Landrace and Large White pig breeds. *Journal of Animal Breeding and Genetics* 139, 695–709. <https://doi.org/10.1111/JBG.12735>.

Schmidt, S., Sasso, E., Vatzia, E., Pierron, A., Lagler, J., Mair, K.H., Stadler, M., Knecht, C., Sperger, J., Dolezal, M., Springer, S., Theußl, T., Fachinger, V., Ladigin, A., Saalmüller, A., Gerner, W., 2021. Vaccination and infection of swine with salmonella typhimurium induces a systemic and local multifunctional CD4+ T-cell response. *Frontiers in Immunology* 11, 603089. <https://doi.org/10.3389/FIMMU.2020.603089/BIBTEX>.

Schrag, T.A., Westhues, M., Schipprack, W., Seifert, F., Thiemann, A., Scholten, S., Melchinger, A.E., 2018. Beyond genomic prediction: combining different types of omics data can improve prediction of hybrid performance in maize. *Genetics* 208, 1373–1385. <https://doi.org/10.1534/GENETICS.117.300374/-DC1>.

Schrauf, M.F., de los Campos, G., Munilla, S., 2021. Comparing genomic prediction models by means of cross validation. *Frontiers in Plant Science* 12, 734512. <https://doi.org/10.3389/FPLS.2021.734512>.

Takagi, Y., Matsuda, H., Taniguchi, Y., Iwaisaki, H., 2014. Predicting the phenotypic values of physiological traits using SNP genotype and gene expression data in mice. *PLOS One* 9, e115532. <https://doi.org/10.1371/JOURNAL.PONE.0115532>.

Tarrés, J., Jové-Juncà, T., Hernández-Banqué, C., González-Rodríguez, O., Ganges, L., Gol, S., Díaz, M., Reixach, J., Pena, R.N., Quintanilla, R., Ballester, M., 2024. Insights into genetic determinants of piglet survival during a PRRSV outbreak. *Veterinary Research* 55, 160. <https://doi.org/10.1186/S13567-024-01421-8>.

Teng, J., Gao, Y., Yin, H., Bai, Z., Liu, S., Zeng, H., Bai, L., Cai, Z., Zhao, B., Li, X., Xu, Z., Lin, Q., Pan, Z., Yang, W., Yu, X., Guan, D., Hou, Y., Keel, B.N., Rohrer, G.A., Lindholm-Perry, A.K., Oliver, W.T., Ballester, M., Crespo-Piazuelo, D., Quintanilla, R., Canela-Xandri, O., Rawlik, K., Xia, C., Yao, Y., Zhao, Q., Yao, W., Yang, L., Li, H., Zhang, H., Liao, W., Chen, T., Karlsson-Mortensen, P., Fredholm, M., Amills, M., Clop, A., Giuffra, E., Wu, J., Cai, X., Diao, S., Pan, X., Wei, C., Li, J., Cheng, H., Wang, S., Su, G., Sahana, G., Lund, M.S., Dekkers, J.C.M., Kramer, L., Tuggle, C.K., Corbett, R., Groenen, M.A.M., Madsen, O., Gòdia, M., Rocha, D., Charles, M., Li, C., Pausch, H., Hu, X., Frantz, L., Luo, Y., Lin, L., Zhou, Z., Zhang, Z., Chen, Z., Cui, L., Xiang, R., Shen, X., Li, P., Huang, R., Tang, G., Li, M., Zhao, Y., Yi, G., Tang, Z., Jiang, J., Zhao, F.,

Yuan, Liu, X., Chen, Y., Xu, X., Zhao, S., Zhao, P., Haley, C., Zhou, H., Wang, Q., Pan, Y., Ding, X., Ma, L., Li, J., Navarro, P., Zhang, Q., Li, B., Tenesa, A., Li, K., Liu, G.E., Zhang, Z., Fang, L., . A compendium of genetic regulatory effects across pig tissues. *bioRxiv* 19, 516073. <https://doi.org/10.1101/2022.11.11.516073>.

VanRaden, P.M., 2008. Efficient methods to compute genomic predictions. *Journal of Dairy Science* 91, 4414–4423. <https://doi.org/10.3168/JDS.2007-0980>.

Visscher, A.H., Janss, L.L.G., Niewold, T.A., de Greef, K.H., 2002. Disease incidence and immunological traits for the selection of healthy pigs. A Review the Veterinary Quarterly 24, 29–34. <https://doi.org/10.1080/01652176.2002.9695121>.

Wade, A.R., Duruflé, H., Sanchez, L., Segura, V., 2022. eQTLs are key players in the integration of genomic and transcriptomic data for phenotype prediction. *BMC Genomics* 23, 1–16. <https://doi.org/10.1186/S12864-022-08690-7/FIGURES/5>.

Wingett, S.W., Andrews, S., 2018. FastQ Screen: a tool for multi-genome mapping and quality control. *F1000Research* 7, 1338. <https://doi.org/10.12688/F1000RESEARCH.15931.2>.